

# The use of Strong Magnetic Field Treatment for Preparation of Proton Exchange Membrane Doped by SeO<sub>2</sub> and its electrochemical properties

Zhengping Zhao<sup>1,2</sup>, Jiajie Hu<sup>2</sup>, Zeping Zhou<sup>2</sup>, Mingqiang Zhong<sup>2,\*</sup>

<sup>1</sup> Zhijiang College, Zhejiang University of Technology, Hangzhou 310014, P.R. China

<sup>2</sup> College of Materials Science and Engineering, Zhejiang University of Technology, Hangzhou 310014, P. R. China

\*E-mail: [mq\\_zhong@163.com](mailto:mq_zhong@163.com)

Received: 4 January 2017 / Accepted: 21 April 2017 / Published: 12 May 2017

---

48% sulfonation degree SPEEK membranes were prepared with rare earth nanoparticles doped and strong horizontal and vertical magnetic field treatment. The experimental results show that the dopant evenly dispersed in the matrix, and took place acid-base pairing interaction with sulfonic acid groups. The interaction of SeO<sub>2</sub> and sulfonic acid group are only occurred in the two-phase interface which has no impact on the crystal structure of doped membrane. After strong magnetic field treatment, the microstructure morphology of doped membrane has no obvious changes. The conductivity of doping modification membrane increased with temperature rising, and reduced with the increase of doping amount. After magnetic field treated, the conductivity of membranes increased significantly, and the vertical direction is obviously superior to the parallel to magnetic field direction. The polar groups take place deformation or re-orientation after processing by strong vertical magnetic field, and form parallel to the film surface of layered distribution, which conduce to the proton transition and prevent the penetration of the methanol molecules. Doping membrane processing by parallel strong magnetic field, polar groups in the membrane re-orientation in vertical plane direction of orientation and form strip random distribution, which is advantageous to the membrane proton in transition.

---

**Keywords:** Electrochemical properties, rare-earth doped, strong magnetic field

## 1. INTRODUCTION

Proton exchange membrane is one of the key components of DMFC [1-4], the performance and prices directly affect fuel cell performance and cost. What materials, kind of solvent or preparation to be used in proton exchange membrane are all should have a high chemical and thermal stability, appropriate mechanical properties and strength, high proton conductivity and methanol permeability

performance. SPEEK membrane has a moderate proton conductivity, high thermal stability and mechanical strength, relatively low cost, and the methanol permeability coefficient is lower than the current commercial fluorine-containing membrane, which is a fluorine-containing proton exchange membrane as an alternative to widespread concern [5-9].

The inorganic and organic polymers prepared membranes can not only maintain the advantages of high temperature inorganic membrane, but also the organic membrane does not make up for the high-temperature corrosion and ease lacking of toughness and can maintain the organic membrane, an inorganic membrane to make up for the lack of brittle, further by changing the membrane structure to reduce methanol permeation. In addition, the polymer material as a carrier which can inhibit the inorganic particles agglomeration and give full play to the advantages of the functional properties of the inorganic particles. Therefore, the organic-inorganic composite membrane performance can be significantly improved [10].

SPEEK has strong polar in the side chains, provides proton-conducting sulfonic acid groups, and there is a strong hydrogen bond acceptor carbonyl groups in the main chain. Therefore, the nano-inorganic materials could be formed van der Waals forces, hydrogen bonding and other physical binding force between SPEEK. It may be connected to forms a covalent bond, achieve composite on the molecular level. The composite membranes which prepared in both toughness and rigid process to ensure more stable mechanical properties of composite membranes, while retaining a high proton conductivity and relatively low methanol permeability [11-12]. Polymer membranes doped by hydrophilic nanomaterials will attract a large number of water molecules and formed water storage areas with sulfonic acid group, to improve heat retention water properties of the membrane material which is conducive to a high temperature proton transport, and improve high-temperature proton conductivity [13].

Strong magnetic field as a special electromagnetic at extreme conditions, high intensity energy could be transferred to the atomic scale matter with non-contact, changing the behavior of arrangement, matching and migration of atoms and molecules, to have a huge and profound impact on the organization and performance of the material [14]. If the volume of grain is large enough, the magnetic field is strong enough, the magnetic anisotropy is greater than thermal fluctuation energy, grain orientation effects will be took placed under the influence of a magnetic field. During the high temperatures manufacturing process, a strong magnetic field is applied to control the orientation of the material grains by using the magnetic anisotropy properties [15]. It is because that the material in different directions of magnetization in a magnetic field, it will produce magnetic energy difference. Under the action of magnetic field orientation, the direction of maximum magnetic susceptibility parallel to the field direction. For the diamagnetic material, the minimum magnetic field of magnetic susceptibility is the direction parallel. The orientation of the magnetic field and material anisotropy of magnetic susceptibility are connected with the size of the magnetic field strength.

Diamagnetic material because of its small magnetic susceptibility, the role of magnetic field to produce has been ignored by people for a long time. In recent years, strong magnetic field applied in the field is increasingly recognized as diamagnetic material due to the development of superconducting technology, non-magnetic body under the 10 T of magnetizing force and 0.01 T under strong magnetic body by magnetizing force quite [16]. Diamagnetism of microcrystalline cellulose dispersed in the

matrix, it can be achieved by strong magnetic fields in the vertical magnetic field direction solidification strengthening polymer matrix at room temperature [17]. Looking at egg dynasty lysozyme and horse spleen ferritin growth under 10T strong magnetic field, it is found that magnetic field can not only change of protein crystal orientation, but also can change the number of crystal protein and transform the shape of the protein crystals and change its quality [17]. In situ polymerization of polyaniline particles prepared by chemical oxidation solution, 10T magnetic field effect on polyaniline grain orientation is not only changed the morphology of polyaniline particles, but also the resistivity of composites was improved [18]. Under the research of diphenyl ketone crystal growth under 0 to 8T magnetic field, it was found that the crystal orientation enhanced performance with the increase of magnetic field, crystals with different magnetic field can follow the boltzmann distribution [19]. Airtight enzyme system in the surface of biological catalysis-biological fuel cells, 0.92 T magnetic field effects increase 3 times battery output power [20]. Brijmohan and Shaw use 0.1 T magnetic field processing  $\gamma$ -Fe<sub>2</sub>O<sub>3</sub> modified sulfonated crosslinked polystyrene proton exchange membrane, membrane conductivity significantly improve [21]. However, it has not seen the modification SPEEK proton exchange membrane through the strong magnetic field.

In this paper, using SeO<sub>2</sub> doped and parallel or perpendicular 8T strong magnetic field treatment the intermediate sulfonation SPEEK (48%) to prepare unary doping proton exchange membrane. To study the relationship of structure and properties of proton exchange membrane, and explore the mechanism.

## 2. EXPERIMENTAL SECTION

### 2.1 The preparation of doping SPEEK membranes

The synthesis if doping proton exchange membrane is consistent with the literature listed [22]. The codes of membranes were described in Table 1.

**Table 1.** Codes of composite membranes specimens

CODE	SPEEK (wt.%)	SeO <sub>2</sub> (wt.%)	Strong Magnetic Field (8T)
SPEEK	100	0	-
SP-S5	95	5	-
SP-S5-PE8	95	5	Perpendicular
SP-S5-PA8	95	5	Parallel
SP-0-PE8	100	0	Perpendicular
SP-0-PA8	100	0	Parallel

### 2.2 Strong magnetic field treatment of the membrane sample

The membranes samples were treated by a strong magnetic field superconducting generator (Superconductor Magnetic Field Instrument, Oxford Instruments, UK) at 8T under 100 °C for 1h.

Processing the membrane plane and the magnetic field direction form an angle of  $90^\circ$  or  $0^\circ$ , like perpendicular or parallel relationship, which are shown in figure 1. Figure 1(b) represents the magnetic field. An arrow indicates the direction of the magnetic field.

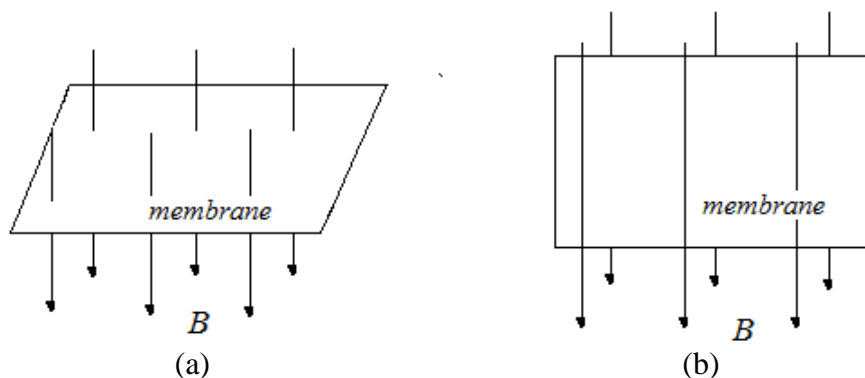


**Figure 1.** Diagram of magnetic vector with surface of membrane, (a) perpendicular, (b) parallel.

The numbers of membranes treated by magnetic field are shown in Table 1, wherein PE represents a strong magnetic field perpendicular to the membrane samples were processed, PA indicates a strong magnetic field parallel to the membrane samples were processed.

### 2.3 The mainly characterization and testing

Fourier transform infrared spectroscopy (FTIR, Nicolet Instruments Nicolet-AVATAR380, USA) is used to characterize the structure of the membranes, and analyze the sample information by OMNIC software.

X-ray Diffractometer (XRD, Regaku D\MAX2250, Japan ) is carried out on the analysis of membrane samples with  $10^\circ\sim 70^\circ$  scanning angle,  $0.02^\circ$  scanning resolution and  $7^\circ/\text{min}$  scanning speed.

Small Angle X ray Scattering (SAXS, Regaku MAX 3000, Japan) is carried out on the analysis of membrane samples with Cu and Ka as radiation source at room temperature with  $0.09^\circ/\text{min}$  scanning speed.  $q$  is scattering wave vector, the scanning range of  $q$  is  $0\sim 0.20\text{\AA}^{-1}$ .

Vibrating sample magnetometer (VSM, LakeShore's 7407-type vibrating sample magnetometer, US) is used to characterize the relationship between the magnetization intensity  $M$  and the magnetic field strength  $H$ , which means using  $M$ - $H$  curve to represent the magnetization characteristics. At room temperature, VSM using an electromagnet magnetic field strength  $H$  is about 1.8 T. The membrane sample is placed in the lower end of the rod vibrating sample compartment, the uniformly strong magnetic field orientation treatment with the test sample by detecting the membrane in the magnetic field direction. In order to accurately characterize the magnetic properties of materials, all test results are diamagnetic signal by subtracting the amount of the test device substrate.

ZL AFM-III AFM atomic force microscope (AFM, Hai Zhuolun using the micro-nano Ltd.) is used to scan in tapping mode collection of information, observe the morphology, and the surface of membrane sample are without any pretreatment.

Proton conductivity of membrane specimens in the traverse direction were measured in a measurement cell using AC Electrochemical Impedance Spectroscopy, which consists of a Solartron Instruments 1287 electrochemical interface and a Solartron Instruments 1255 B frequency response analyzer (UK). The EIS recorded over a frequency range of 1-10<sup>6</sup> Hz. Before the tests, all membrane specimens were abundantly immersed in 1mol/L hydrochloric acid solution for 24 h then rinsed with de-ionized water several times. Consequently, resistance of membranes was measured and proton conductivity was calculated as described. [17]

### 3. RESULTS AND DISCUSSION

Using the Nicolet-AVATAR380 to analyze SP and SP-S5 membrane samples at room temperature, and obtained FT-IR spectra are shown in figure 2. To SP samples, 1020 cm<sup>-1</sup> corresponding to S=O bond stretching absorption peaks, 1079 cm<sup>-1</sup> corresponding to O=S=O bond symmetric stretching vibration, 1240 cm<sup>-1</sup> corresponding to O=S=O asymmetric stretching vibration, 1260 cm<sup>-1</sup> corresponding to -Ar-O- group peaks, 1642 cm<sup>-1</sup> corresponding to -Ar-C(=O)-Ar- group peaks. In the SP-S5 samples, there are 1252 cm<sup>-1</sup> stretching absorption peak, which may be -O- bond peak has shifted due to the doped of rare earth oxide SeO<sub>2</sub>. SeO<sub>2</sub> has a strong infrared absorption peak at 400 cm<sup>-1</sup> and a weak infrared absorption peak of near 700 cm<sup>-1</sup>. Therefore, the 422 cm<sup>-1</sup> characteristics peak in SP-S5 sample may be SeO<sub>2</sub>. The wave crest move to the high number of direction which is due to nanometer SeO<sub>2</sub> took place acid-base pairing interaction with sulfonic groups and caused action blue shift, but weak infrared absorption peak does not appear in the spectra.

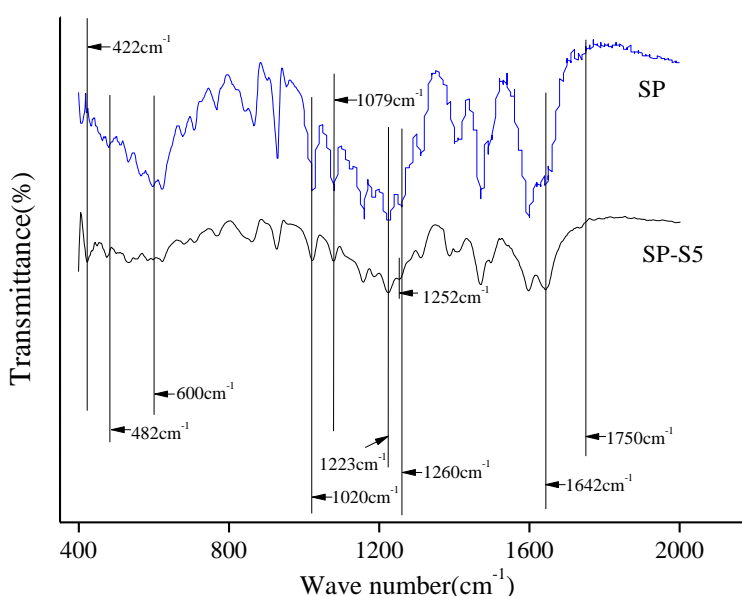


**Figure 2.** The FT-IR spectra curves: SP, SP-S5

Using D\max 2550 X-ray diffraction analysis SP, SP-S5, SP-S5-PE8 and SP-S5-PA8 membrane samples doped by  $\text{SeO}_2$  and strong magnetic field to obtain XRD spectra, which are shown in figure 3.

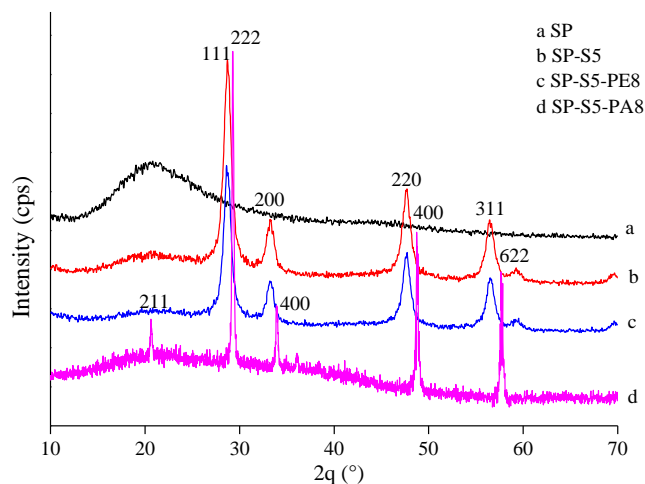


**Figure 3.** XRD pattern of membrane specimens: SP, SP-S5, SP-S5-PE8, SP-S5-P8

SP48 membrane sample is typical amorphous diffraction peak [9], The diffraction peaks (111), (200), (220), (311) and (222) of membrane sample SP-S5 and SP-S5-PA8 are corresponding agreement to  $\text{SeO}_2$  diffraction peak position, indicating that the doped membrane containing  $\text{SeO}_2$  crystal structure and free from 8T strong magnetic field parallel processing effects [23].  $\text{SeO}_2$  and sulfonic acid groups form a coordination in the occurrence of the two-phase interface, membrane doped crystal structure is not affected or the occurrence of weak internal membrane changes are not reflected in the characteristic diffraction peaks. Doped membrane FWHM becomes larger, which compared to show that SP48 membrane doped membrane structure becomes denser.

Using D\max2550 X-ray diffractometer to analysis crystal structure of SP-S5 membrane doped by  $\text{SeO}_2$  and soaking by hydrochloric acid to obtain XRD spectra which are shown in figure 4.

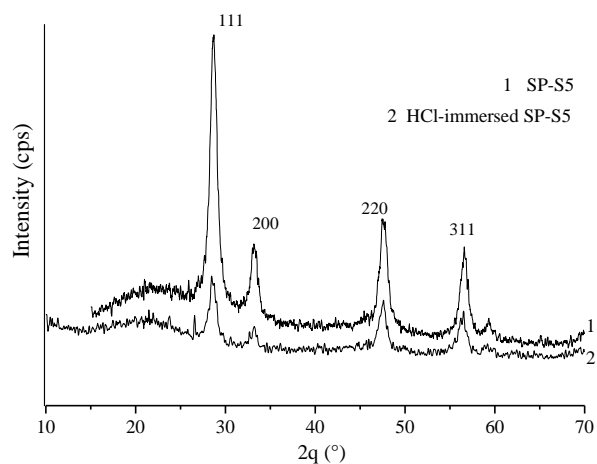


**Figure 4.** XRD pattern of membrane specimens

Doping SeO<sub>2</sub> membrane was soaked in hydrochloric acid, the diffraction peak position has no significant change, but the diffraction intensity becomes relatively weak. SPEEK is amorphous polymer which having diffraction peaks typical broad peak. Because of the SeO<sub>2</sub> crystal structure stored in the doped membrane, the membrane appears SeO<sub>2</sub> characteristic peaks. After soaking hydrochloric acid solution of doped membrane, due to its crystal structure were not changed or altered too weak which do not cause significant changes in the structure. It is indicated that the coordination role of SeO<sub>2</sub> and SPEEK only occur in two solid interfaces, whether or not soak hydrochloric acid were not effect of SeO<sub>2</sub> crystal structure within the membrane.

Using SAXS MAX 3000 small-angle X-ray scattering instrument to analyze the membranes and crystal structures passed through 8T vertical or parallel magnetic field treatment. To obtain SAXS spectra of SP, SP-0-PE8 and SP-0-PA8, which are shown in figure 5.

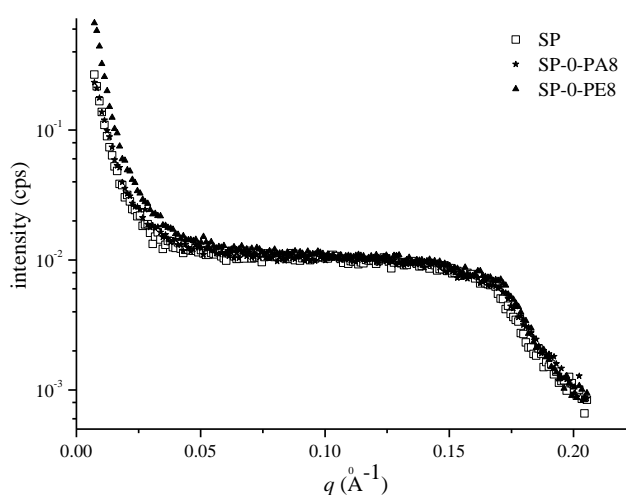


**Figure 5.** SAXS spectrogram of membrane specimens: SP, SP-PA8, SP-PE8

From the spectrogram, three membrane samples are all have a same broad peak at  $0.1727\text{\AA}^{-1}$ , but there was no apparent shoulder. Without or treatment by magnetic field process, SAXS spectrum of the SP sample are substantially the same. It is indicated that the magnetic force of the SP in the polar group is relatively weak. The 8T strong magnetic field treatment has no significant changes in its internal structure or undergone minor changes failed to find by SAXS characterization. In addition, the direction change of magnetic field treatment did not affect in the scattering peak intensity [24].

Using SAXS MAX 3000 small-angle X-ray scattering instrument to analyze membranes doped SeO<sub>2</sub> and crystal structures through 8T parallel processing magnetic field to obtain SAXS spectra of SP, SP-0-PA8, SP-0-PE8, SP-S5 and SP-S5-PA8. The curves are shown in figure 6. Five samples are all have one same broad peaks at  $0.1685\text{\AA}^{-1}$ , SP, SP-S5, SP-S5-PA8 samples have a common shoulder  $0.1854\text{\AA}^{-1}$  in place, but SP-S5 and SP-S5-PA8 shoulder sample was in  $0.1874\text{\AA}^{-1}$  at the value increases to q direction, orientation or alignment membrane show polar groups in a strong magnetic field and doping processing volume impact of doping within 5wt.% of insufficient volume doped significant changes in the SAXS spectrum, which contain 8wt.% of SeO<sub>2</sub> doped membrane after 8T parallel

magnetic field, the spacing membrane polar groups are slightly smaller, causing scattering peak to increase the wave vector direction of movement.

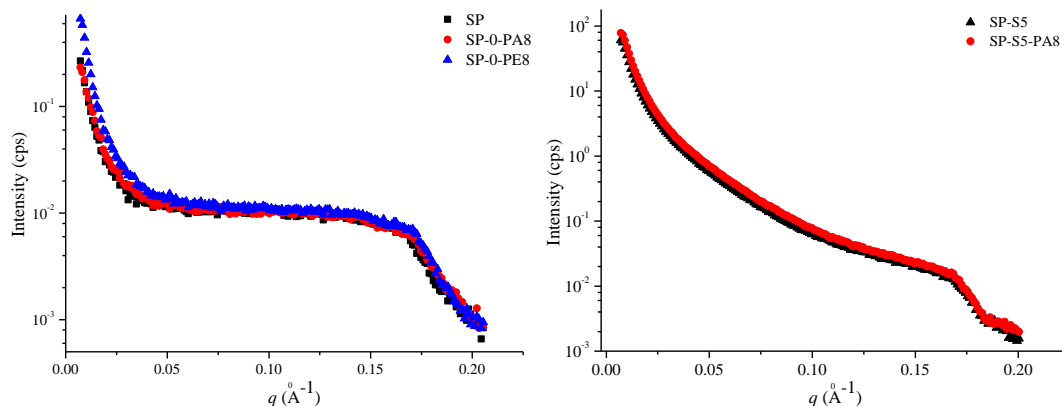


**Figure 6.** SAXS profile of different specimens treated with high magnetic field

After SeO<sub>2</sub> doping SPEEK, magnetic force doped membrane role was significantly increased, so that the membrane changes occur orderly polar groups, the structure becomes dense. Figure 6 peak position has not changed, it may not be significant changes in the crystal structure, or occur only on two solid interface does not cause a change in the internal structure of the polar group spacing or slightly change not visible in the XRD, and SP-S5-PA8 shoulder of samples is offset, indicating that structural changes be displayed on the SAXS. SP-S5 and SP-S5-PA8 sample SP and SP-S5-PA8 slightly larger than the relative strength of the sample, which showed that magnetic field treatment on doping respond somewhat different from the undoped SP again Thus, the strength of the magnetic field magnitude and direction were not affected.

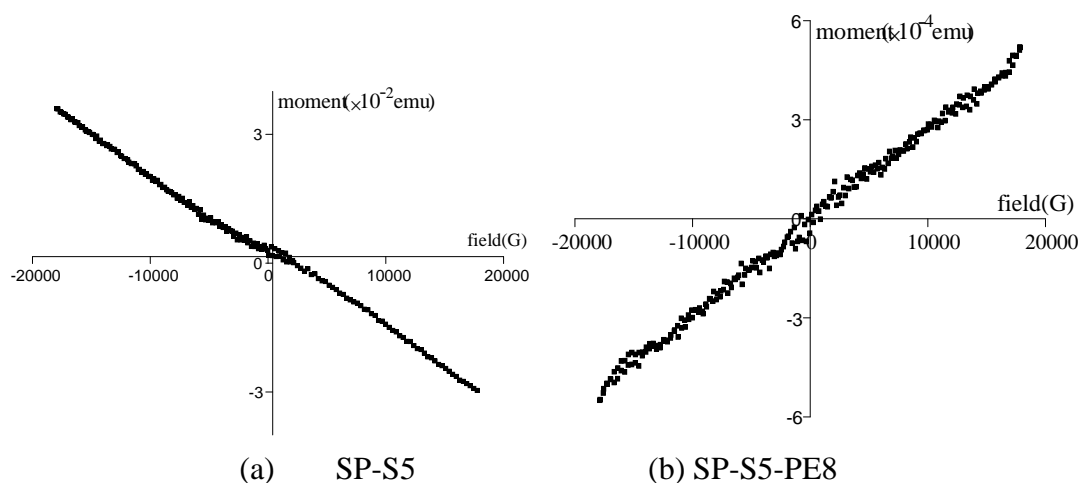


**Figure 7.** M-H curve of membrane specimens

At room temperature using 7407-type vibrating sample magnetometer (Vibrating Sample Magnetometer, VSM), detecting the magnetization curve different SeO<sub>2</sub> doping and magnetic membrane sample processing, characterization of the membrane material in which the magnetization

M of the magnetic field strength H relations, reflecting the magnetization characteristics of the membrane material. Since the SP-S5 and SP-S5-PE8 two samples showed diamagnetic, so I chose only SP-S5 as a representative sample, and showed a paramagnetic SP-S5-PE8 comparative sample, get their MH curve shown in figure 7.

From figure 7, it is show that the membrane samples of rear SPEEK incorporation SP-S5 doped by  $\text{SeO}_2$  still showed diamagnetic. MH curves of SP-S5-PE8 with perpendicular or parallel direction 8T strong magnetic field treatment are still diamagnetism. It could be that the membrane may be doped grain size is not large enough, and the magnetic anisotropy energy is less than thermal fluctuation energy. The grains of a magnetic field is difficult orientation effects occur or occur relatively weak orientation effects on the magnetization curve but difficult to find. In figure 7(b), SP-S5-PE8 membrane sample is manifested weakly paramagnetic with the vertical direction after 8T strong magnetic field treatment. It is may be the grain of 5 wt.% doping has a certain volume and 8T magnetic field strength is large enough, which lead to the magnetic anisotropy energy greater than the thermal fluctuation energy. The grain occur orientation effects under the magnetic field, so that the membrane manifest a paramagnetic sample performance.

SPEEK is diamagnetic material. The electron magnetic moments of atomic cancel each other, and co-zero the magnetic moment [25]. When subjected to strengthen with external magnetic field, the electron orbit games change and produce a small magnetic moment together with the applied magnetic field in the opposite direction, which showing a negative diamagnetic susceptibility. After 8T strong magnetic field treatment, doping produces not fully offset the electronic magnetic moments of atoms or molecules in the membrane. But no strong magnetic moment between atoms or molecules interact in a hot chaotic commotion arranged by atomic magnetic moment magnetic field magnetic field tends to make the arrangement, the overall effect is a certain magnetic moment component in the direction of the applied magnetic field so that the magnetic susceptibility values become small positive value, therefore. SP-S5-PE8 samples showed weak paramagnetic. Visible, special magnetic  $\text{SeO}_2$  doped diamagnetic material SPEEK later, under strong magnetic field can change the orientation of the polar group alignment membrane, causing the doped membrane properties change. But insufficient or no doping  $\text{SeO}_2$  samples by magnetic field of sufficient strength.

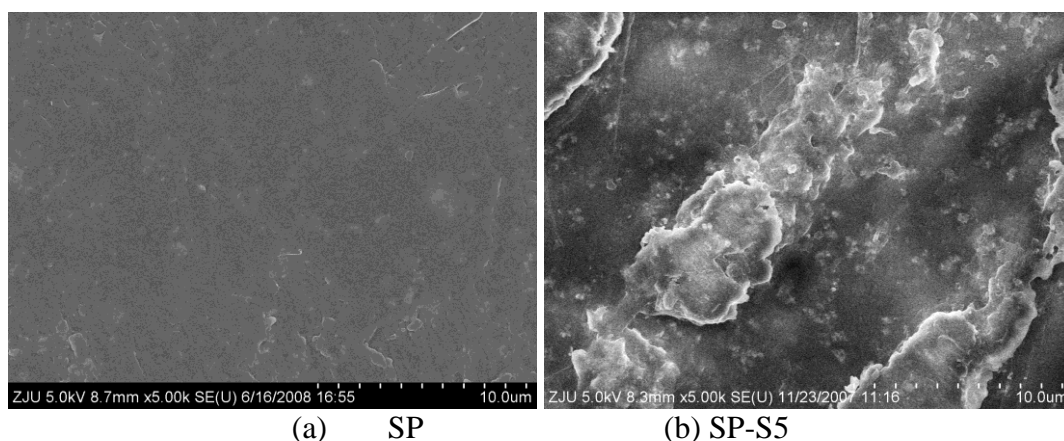


**Figure 8.** SEM surface of membrane specimens

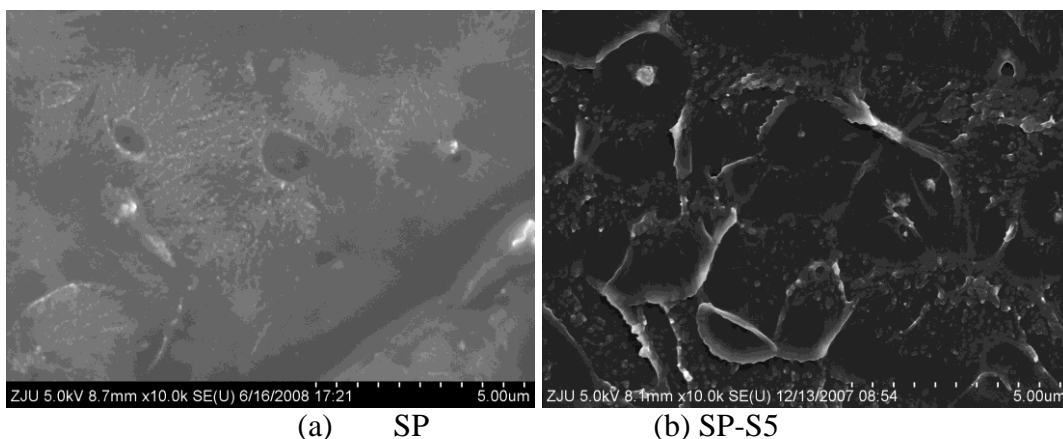


Figure 9. SEM cross-section of different membrane specimens

The more difficult to find on the characterization of the change, SAXS analysis also proved this conclusion. The membrane samples were treatment at 8T powerful magnetic field treatment after 4h and probably during the rotation through domain wall displacement and magnetic domains, which causing irreversible domain wall displacement and irreversible movement, temperature rise helps irreversible susceptibility. So, the membrane samples were strong after the magnetic field treatment is not significantly affected by storage time.

Using HITACHI S-4800 scanning electron microscope (Scanning Electron Microscopy, SEM), and the membrane was observed by the pure SPEEK 5wt.% SeO<sub>2</sub> doped sample membrane, thereby obtaining an SEM SP and SP-S5 surface of the membrane sample morphology figure 8 and fracture surface shown in figure 9.

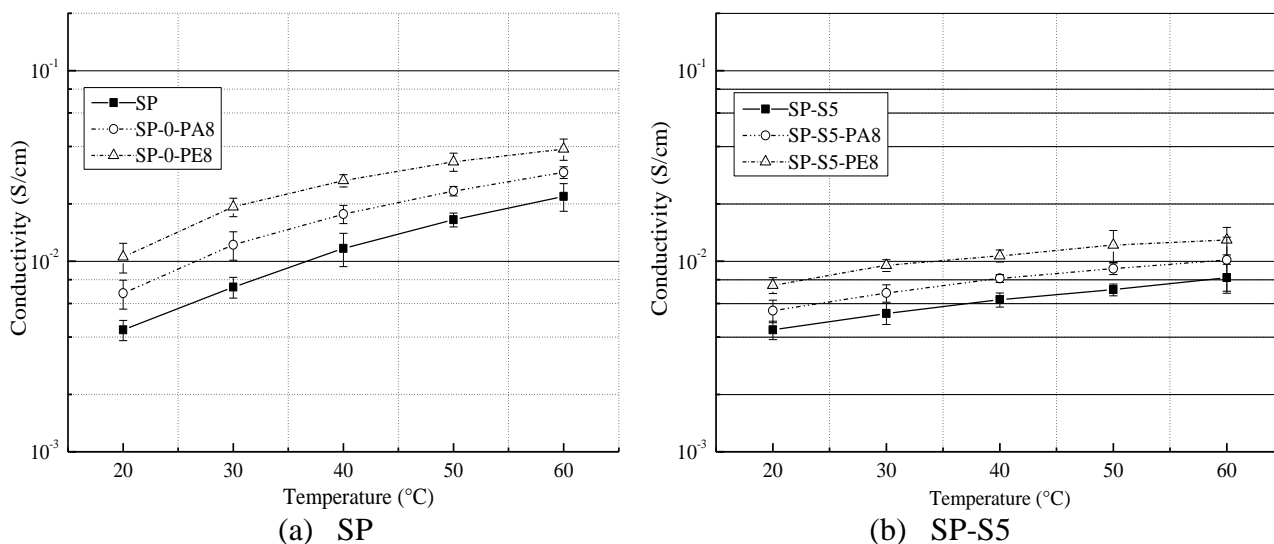


Figure 10. The conductivity of membrane specimens with different high magnetic field treatment

From the pictures, it is indicated that the SP membrane sample surface are smooth, no cracks, no grooves and holes. SP-S5 membrane surface has more prominent streaks, which may cause local accumulation of membrane solution casting process. Two membrane samples showed no obvious

phase separation, indicating dense material. Fracture of the membrane sample no obvious contrast and large white border brittle fracture neat, which indicating that the fault level and the sample is amorphous material [26]. SP sample has no cross-section mesh structure, but the presence of pits. It is probably due to the deposition of thin membrane molecular force action. SP-S5 has fault large flake resin may SPEEK clusters and small particles from the particle size analysis may  $\text{SeO}_2$  and SPEEK mixture. There are no network structure, holes and pores, no nano- $\text{SeO}_2$  in the membrane into large aggregates clumps, all above indicating that the doped membrane section nano- $\text{SeO}_2$  dispersed more evenly.

Testing unprotonated SP membrane and  $\text{SeO}_2$  doping resistance membrane by a strong magnetic field before and after treatment, and the result curves of conductivity with temperature are shown in figure 10.

The conductivity three membrane samples were gradually increased with increasing temperature, SP membrane conductivity higher than  $40^\circ\text{C}$  were higher than  $10^{-2}\text{S/cm}$ . The membrane samples after magnetic field treatment, which significantly improve electrical conductivity, electrical conductivity through conductivity vertical processing membrane sample than in a direction parallel processing of large, indicating strong magnetic field perpendicular to the direction of proton exchange membrane sample processing to improve the membrane conductivity more effective [27].

With the increase of  $\text{SeO}_2$  doping amount of doped membrane conductivity decreased gradually in the corresponding temperatures, may be doped  $\text{SeO}_2$  interact with a sulfonic acid group participation leads to proton conduction number of sulfonic acid groups decreased. The membrane samples were 6T strong magnetic field parallel or perpendicular to the direction of the process, the conductivity in the test temperature range reached  $10^{-2}\text{S/cm}$ , and at a temperature of  $20^\circ\text{C}$  and  $30^\circ\text{C}$ , SP-S5-PE8 conductivity membrane conductivity of the sample than SP48 large. From figure 10(b), the membrane is a strong magnetic field parallel to the sample after treatment, the conductivity was improved to a lesser extent. SP-S5-PA8 and proton conductivity SP-PE8 membrane samples in the temperature range of the test did not reach the  $10^{-2}\text{S/cm}$ . The conductivity of SP-S5-PE8 membrane sample increase by a big margin, 20 and  $30^\circ\text{C}$  greater than SP membrane sample close  $10^{-2}\text{S/cm}$  at  $50^\circ\text{C}$ , but more than  $60^\circ\text{C}$ .

The membrane samples after magnetic field treatment, the conductivity of the membrane sample by vertical processing at a temperature of  $\leq 30^\circ\text{C}$  than SP conductivity of large, more than  $10^{-2}\text{S/cm}$  in the test temperature. In addition to the SP-S5-PA8 sample conductivity which row direction of the process of a membrane sample in a test temperature reached  $10^{-2}\text{S/cm}$ , showed a strong magnetic field on the membrane polar groups play orientation or deformation role to contribute to the proton conducting membrane. At the same time, we found that the amount of  $\text{SeO}_2$  doping increases the electrical conductivity of the membrane sample with increasing temperature decreased sensitivity may doping can increase the thermal stability of the membrane.

Two different dielectric membrane conductivity were test to evaluate SP and SP-S5 membrane samples in 1 mol/L hydrochloric acid solution and 95% RH the water vapor, and the resulting conductivity varies with temperature curves are shown in figure 11. In figure 11(a), the conductivity of the sample both membranes were increased with increasing temperature in an acid solution of the test medium. The conductivity of the SP-S5 sample conductivity is 15 times higher than SP sample

approximately. The results are more than  $10^{-2}$  S/cm in the range of 20-60 °C, and more than  $10^{-1}$  S/cm above 30 °C. The conductivity of SP membrane is also more than  $10^{-2}$  S/cm at 60 °C. In the water vapor medium, the membrane conductivity was increased with increasing temperature. SP membrane sample conductivity are more than  $10^{-2}$  S/cm in the range of 20-60 °C, and the electrical conductivity of the SP-S5 sample are close to but did not reach  $10^{-2}$  S/cm, about 40% of SP membrane conductivity.

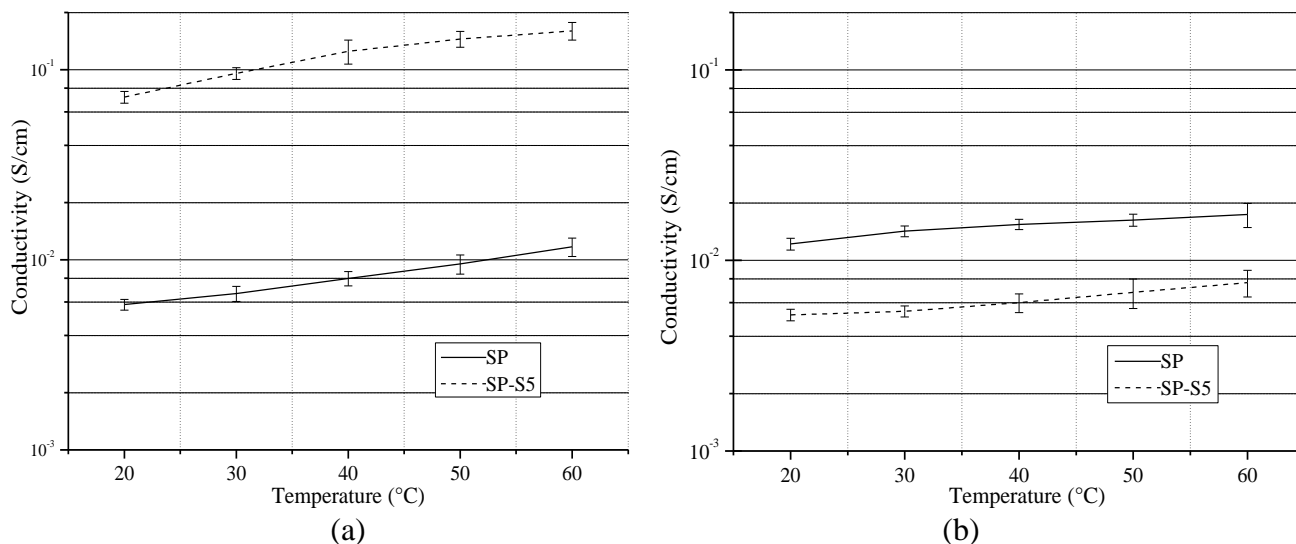
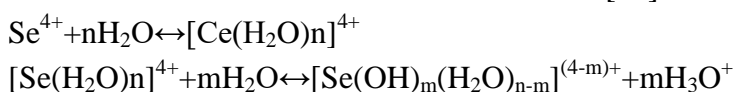


**Figure 11.** Conductivity of membrane specimens in different media as a function of temperature: (a) HCl solution and (b) water vapour

The conductivity of SP and SP-S5 membrane samples in two different media increased with the temperature increasing, which are mainly due to the membrane sulfonic acid groups attract water molecules formed around the micro-aqueous phase. Sulfonic acid group effective spacing becomes smaller, and the proton activity increased with increasing temperature. Thus, improving the proton in the transition between the ability of a sulfonic acid group, proton-rich acid medium conducive to the proton conductivity. However, SP conductivity than water vapor medium acid medium is large, the gap may be due to a factor in acid medium and the membrane electrode in an acid solution. The resulting of interfacial resistance, so that the conductivity of the membrane is reduced. Another factor, the morphology of the membrane is no obvious network structure, pores and channels, membrane proton may not primarily by the medium solution through the membrane channel geometry passing thought, but mainly through the membrane hydrophilic sulfonic acid groups in the transition between the conduct. SP-S5 conductivity of the sample in an aqueous medium than low purity steam SP sample, the reason is SeO<sub>2</sub> and sulfonic acid groups acid-base complex, reducing the number of sulfonic acid groups involved in conducting protons to a certain extent resulting in conductivity of the sample was only 40% SP. In acid solution medium, SP-S5 sample appeared opposite variation and mainly due to SeO<sub>2</sub> has a special redox environment in an acid solution. The nano-SeO<sub>2</sub> following reversible reaction occurs in an acid solution medium [28].





In an acid solution medium, although these reactions is a reversible dissolution equilibrium, but the inner and outer membrane proton-rich samples favors the formation of an effective proton conductivity, good for proton transitions between the sulfonic acid group. Thus, the incorporation of nano-SeO<sub>2</sub> modified SPEEK membrane conductivity in acid solution medium significantly increased 15 times greater than the electrical conductivity of pure SP membrane. However, since the sulfonic acid group in a high electron density of the benzene ring linked pair ether bond, an ether bond under acidic conditions due to the induction of a sulfonic acid group ortho-position becomes unstable, resulting in a polymer chain breakable reduce the chemical stability of the polymer and doped membranes used in the acidic environment of the need to be careful.

#### 4. CONCLUSIONS

Preparation of SeO<sub>2</sub> doped DS of 48% SPEEK membrane, dopants are more evenly dispersed in SPEEK matrix and the sulfonic acid groups in SPEEK acid-base complex role. SeO<sub>2</sub> interaction with the sulfonic acid group occurs only in two solid interface, which do not affect the membrane doped crystal structure, and unaffected after soak by 1mol/L hydrochloric acid. After a strong magnetic field treatment, the membrane morphology did not significantly change doped by SeO<sub>2</sub>. Through 8T strong magnetic field perpendicular to the direction of processing, SP-S5-PE8 membrane sample is manifested weakly paramagnetic. Strong magnetic field and doping content are not significantly change the surface morphology of SeO<sub>2</sub> doped membrane. The conductivity of SeO<sub>2</sub> doped membrane increased with the temperature increasing, decreased with the doping content. After a strong magnetic field treatment, the conductivity of the membrane significantly improved. The perpendicular direction is significantly better than the parallel direction.

#### ACKNOWLEDGEMENTS

We are thankful for the National Natural Science Foundation of China (No. 21504079) and Project Supported by Zhejiang Provincial Natural Science Foundation of China (Grant No. LQ14E030004) for the support to this research.

#### References

1. B. Suleiman, A.S. Abdulkareem, U. Musa, I.A. Mohammed, M.A. Olutoye and Y.I. Abdullahi, *Energ. Convers. Manag.*, 117 (2016) 228.
2. Z.P. Zhao, Z.P. Zhou and M.Q. Zhong, *Int. J. Electrochem. Sci.*, 10 (2015) 5880.
3. P. Bhavani and D. Sangeetha, *Energy*, 36 (2011) 3360.
4. L. Gubler, *Adv. Energy Mater.* 4 (2015) 1.
5. M.M. Radhi, W.T. Tan, M.Z. Rahman and A.B. Kassim, *Int. J. Electrochem. Sci.*, 5 (2010) 254.
6. O. Kyeongmin and J. Hyunchul, *Int. J. Hydrogen Energ.* 29 (2015) 7743.
7. Y. He, L. Geng, C.Y. Tong, L.D. Liu and C.L. Liu, *Polym. Inter.* 63 (2014) 1806.
8. Z.P. Zhao, Z.P. Zhou and M.Q. Zhong, *Int. J. Electrochem. Sci.*, 9 (2014) 8120.

9. Suzuki Takahiro, Hashizume Ryohei and Hayase Masanon, *J. Power Sources*, 15 (2015) 109.
10. Z.P. Zhao, Z.P. Zhou and M.Q. Zhong, *Int. J. Electrochem. Sci.*, 10 (2015) 5026.
11. S.D. Mikhailenko, S.M.J. Zaidi and S. Kaliaguine, *J. Polym. Sci. Pol. Phys.*, 38 (2000) 1386.
12. P.X. Xing, G.P. Robertson, M.D. Guiver and X.G. Jian, *J. Membrane Sci.*, 229 (2004) 95.
13. J. Lee and C.S. Marvel, *J. Polym. Sci. Pol. Chem.*, 22 (1984) 295.
14. M. Matsuguchi and H. Takahashi, *J. Membrane Sci.*, 281 (2006) 558.
15. E. Zygadlo-Monikowska, Z. Florjanczyk, E. Wielgus-Barry and E. Hildebrand, *J. Power Sources*, 159 (2006) 392.
16. V.R. Hande, S.K. Rath, S. Rao and M. Patri, *J. Membrane Sci.*, 372 (2011) 40.
17. Z.P. Zhao, J.J. Hu, Z.P. Zhou and M.Q. Zhong, *Optoelectron. Adv. Mat.*, 10 (2016) 117.
18. R. Naresh Muthu, S. Rajashabala and R. Kannan, *Int. J. Hydrogen Energ.*, 34 (2009) 7919.
19. S. Jian, L. Guang and Q. Jin, *Electrochim. Acta*, 20 (2015) 174.
20. S.R. Rubero and S. Baldelli, *J. Phys. Chem. B*, 110 (2006) 4756.
21. J.K. Lee, W.Li and A. Manthiram, *J. Power Sources*, 180 (2008) 56.
22. A. Mokrini and M.A. Huneault, *J. Power Sources*, 154 (2006) 51.
23. C.A. Idibie, A.S. Abdulkareem, H.C. Pienaar, S.E. Iyuke and L. Vandyk, *J. Appl. Polym. Sci.*, 166 (2010) 3474.
24. L.J. Hobson, H. Ozu, M. Yamaguchi and S. Hayase, *J. Electrochem. Soc.*, 148 (2001) 28.
25. T. Kang, M.J. Kim, J.T. Kim and Y.J. Sohn, *Int. J. Hydrogen Energ.*, 27 (2015) 5444.
26. S. Cuynet, A. Cailard, S. Kaya-Boussougou, T. Lecas, N. Semmar, J. Bigarre, P. Buvat and P. Brault, *J. Power Sources*, 1 (2015) 299.
27. C.H. Shen, Z.H. Guo, C. Chen and S.J. Gao. *J. Appl. Polym. Sci.*, 126 (2012) 954.
28. H. Gu and M.D. Soucek, *J. Chem. Mater.*, 19 (2007) 1103.

© 2017 The Authors. Published by ESG ([www.electrochemsci.org](http://www.electrochemsci.org)). This article is an open access article distributed under the terms and conditions of the Creative Commons Attribution license (<http://creativecommons.org/licenses/by/4.0/>).